

Published in final edited form as:

Circ Cardiovasc Imaging. 2013 July ; 6(4): . doi:10.1161/CIRCIMAGING.113.000528.

Aortic Dilation in Bicuspid Aortic Valve Disease: Flow Pattern Is a Major Contributor and Differs with Valve Fusion Type

Malenka M. Bissell, MD, BM, MRCPCH¹, Aaron T. Hess, PhD¹, Luca Biasioli, DPhil¹, Steffan J. Glaze¹, Margaret Loudon, MBChB, MRCP¹, Alex Pitcher, BMBCh, MRCP¹, Anne Davis, BSc Hons¹, Bernard Prendergast, DM, FRCP, FESC², Michael Markl, PhD³, Alex J. Barker, PhD³, Stefan Neubauer, MD, FRCP, FACC, FMedSci¹, and Saul G Myerson, MB ChB, MD, MRCP, FESC^{1,2}

¹University of Oxford Centre for Clinical Magnetic Resonance Research (OCMR), Division of Cardiovascular Medicine, Radcliffe Department of Medicine, Oxford, United Kingdom

²Department of Cardiology, John Radcliffe Hospital, Oxford, United Kingdom

³Department of Radiology, Northwestern University Feinberg School of Medicine, Chicago, IL

Abstract

Background—Ascending aortic dilation is important in bicuspid aortic valve disease (BAV), with increased risk of aortic dissection. We used cardiovascular magnetic resonance (CMR) to understand the pathophysiology better by examining the links between 3-dimensional flow abnormalities, aortic function and aortic dilation.

Methods and Results—142 subjects underwent CMR (mean age 40 years; 95 with BAV, 47 healthy volunteers [HV]). BAV patients had predominantly abnormal right-handed helical flow in the ascending aorta, larger ascending aortas (18.3 ± 3.3 vs. 15.2 ± 2.2 mm², $p < 0.001$), and higher rotational (helical) flow (31.7 ± 15.8 vs. 2.9 ± 3.9 mm²/s, $p < 0.001$), systolic flow angle (23.1 ± 12.5 vs. $7.0 \pm 4.6^\circ$, $p < 0.001$) and systolic wall shear stress (WSS) (0.85 ± 0.28 vs. 0.59 ± 0.17 N/m², $p < 0.001$) compared to HV. BAV with right-handed flow and right-non coronary cusp fusion ($n = 31$) showed more severe flow abnormalities (rotational flow 38.5 ± 16.5 vs. 27.8 ± 12.4 mm²/s, $p < 0.001$; systolic flow angle 29.4 ± 10.9 vs. $19.4 \pm 11.4^\circ$, $p < 0.001$; in-plane WSS 0.64 ± 0.23 vs. 0.47 ± 0.22 N/m², $p < 0.001$) and larger aortas (19.5 ± 3.4 vs. 17.5 ± 3.1 mm², $p < 0.05$) than right-left cusp fusion ($n = 55$). BAV patients with normal flow patterns had similar aortic dimensions and WSS to HV and younger BAV patients showed abnormal flow patterns but no aortic dilation, both further supporting the importance of flow pattern in the etiology of aortic dilation. Aortic function measures (distensibility, aortic strain and pulse wave velocity) were similar across all groups.

Conclusions—Flow abnormalities may be a major contributor to aortic dilation in BAV. Fusion type affects the severity of flow abnormalities, and may allow better risk prediction and selection of patients for earlier surgical intervention.

Keywords

bicuspid aortic valve; aorta; wall shear stress; vascular function; cardiac magnetic resonance imaging

Correspondence to: Dr. Malenka Bissell, University of Oxford, OCMR, Level 0, John Radcliffe Hospital, Headley Way, Oxford, OX3 9DU, United Kingdom, Phone: +44 1865 221875, Fax: +44 1865 740449, malenka.bissell@cardiov.ox.ac.uk.

Disclosures

None.

Bicuspid aortic valve disease (BAV) is the most common congenital heart disorder with a prevalence of 1-2%.¹ Up to 80% of patients with BAV develop ascending aortic dilation, with important clinical sequelae including a nine-fold increased risk of aortic dissection.¹ There is considerable debate regarding the etiology of the aortic dilation.² While some suggest an intrinsic aortic wall pathology,³ there is increasing evidence that hemodynamic flow abnormalities in the proximal aorta caused by the BAV are at least partially responsible.⁴ The aortopathy may also vary between different types of BAV fusion - recent animal studies suggest that these may be different genetic entities,⁵ and a small retrospective echocardiographic study showed reduced aortic root distensibility in the RL-BAV group but no difference in the ascending aorta.⁶

Understanding the etiology of aortic dilation in BAV is important for risk prediction and potential intervention in the future. Recent developments in cardiovascular magnetic resonance (CMR) have facilitated the measurement of time-resolved 3-dimensional flow patterns ('4D flow'), in addition to the detailed aortic size and function assessments available previously. Two recent CMR studies have examined flow patterns in BAV, mainly focusing on the commoner right-left coronary cusp fusion type (RL-BAV), and showed a markedly eccentric increased wall shear stress (WSS) distribution.^{7, 8} There were no data on aortic vascular function, however, and only concerning few patients with the right-non coronary cusp fusion (RN-BAV) type.

Our study aims to examine in more detail the links between flow patterns, aortic dilation and measures of aortic vascular function using CMR to 1) understand the pathophysiological mechanisms of aortic dilation in BAV and 2) identify novel markers for disease progression and the risk of aortic dilation. We also aimed to compare the two most common BAV fusion types (RL-BAV and RN-BAV) with larger numbers of each than previously examined, to determine any differences in flow patterns, aortic size and function and whether these represent different disease phenotypes which could be used for risk stratification. Finally, we examined pediatric patients to identify flow and aortic function changes before or at an early stage of aortic dilation to gain a better understanding of the causes of aortic dilation and pathophysiology at different stages of the disease process.

Methods

Patient recruitment

Patients with bicuspid aortic valves were recruited prospectively from cardiology clinics and CMR lists between January 2011 and November 2012. Patients with complex congenital heart disease were excluded. We also excluded one BAV patient with aortic root dilation alone (with normal sized ascending aorta), as this is thought to be a separate inherited condition, in association with BAV.⁴ Three patients with fully repaired coarctation of the aorta and one patient with an incidental small atrial septal defect were included. Our healthy volunteers were recruited from posters within the hospital and University buildings, and were free from any known significant medical problems. The healthy volunteers were age and sex-matched at time of recruitment. The study was approved by the West Berkshire ethics committee and all participants or their guardians gave written informed consent.

Cardiovascular magnetic resonance acquisition

Each subject underwent two CMR scans – one on a 1.5 Tesla system (Avanto, Siemens, Erlangen, Germany) for anatomical imaging; the second on a 3.0 Tesla system (Trio, Siemens, Erlangen, Germany) for 4D flow assessment, both using a 32-channel cardiac coil. All images were electrocardiogram (ECG)-gated. Steady-state free-precession (SSFP) cine sequences acquired during a single breath-hold were used for aortic dimension

measurements, left ventricular volume assessment and aortic valve morphology. Valve morphology was classified by leaflet fusion type.⁹ Short axis planes of the aorta were acquired perpendicular to the long axis at the sinuses of Valsalva, sino-tubular junction, ascending and proximal descending aorta at the level of the pulmonary artery, and a further plane in the descending aorta 12cm below the first plane. For aortic function measures (distensibility and maximal rate of systolic distension), free-breathing SSFP images with a high temporal resolution (10ms)¹⁰ were acquired in the same short axis aortic planes as for dimensions (latter three above). Through-plane phase contrast velocity mapping images with a high temporal resolution were acquired perpendicular to the ascending and descending aorta at the level of the pulmonary artery for pulse wave velocity (PWV) calculations.

Aortic diameters were measured from inner edge to inner edge at end-diastole; diameters of the sinuses were measured from cusp to commissure.¹¹ All aortic diameters were indexed for body surface area (BSA) using the Haycock formula¹² to account for the wide range of body size and relatively smaller diameters in the pediatric subjects. The velocity across the aortic valve was measured using through-plane phase contrast velocity mapping in an image slice placed perpendicular to the ascending aorta, just above the valve tips. Aortic stenosis was defined as absent or mild if peak velocity was <3m/s, and moderate-severe if ≥ 3 m/s. CMR42 (Circle Cardiovascular Imaging Inc., Calgary, Canada) was used for analysis of standard anatomical and velocity parameters and customized Matlab software Version R2010a (The MathWorks Inc, Natick, Massachusetts, USA) for vascular measures. Central blood pressure (for aortic distensibility) was measured during the CMR scan using the Vicorder device (Smart Medical, Moreton in Marsh, United Kingdom), calibrated to brachial cuff pressures.¹³

4D flow assessment

Flow-sensitive gradient-echo pulse sequence CMR was used to characterize and quantify flow hemodynamics in the thoracic aorta. Datasets were acquired with prospective ECG-gating during free-breathing, using a respiratory navigator. The image acquisition volume was in an oblique sagittal plane encompassing the whole thoracic aorta. Sequence parameters: echo time 2.5ms, repetition time 5.1ms, flip angle 7°, voxel size 1.9-2.0×1.5-1.7×2.0-2.2mm³, temporal resolution 40ms. The velocity encoding range was determined using the lowest non-aliasing velocity on scout measurements (healthy volunteers 1-1.5m/s; BAV patients 1.5-4.5m/s). Dataset processing and WSS calculation were conducted with customized Matlab software Version R2010a (The MathWorks Inc, Natick, Massachusetts, USA) and EnSight Version 9.1.2 (CEI Inc, Apex, North Carolina, USA), as described previously.^{8, 14-16}

Helical blood flow and wall shear stress quantification

Flow through the ascending aorta in normal subjects is usually cohesive, with a slight helical spiral, though in BAV patients the flow has been shown to be highly deranged with markedly accentuated helical flow.¹⁷ Helical flow is composed of a forward component (along the long axis of the aorta) and a rotational component (rotating around the long axis in a circumferential direction). The 3-dimensional flow patterns were measured in a short axis slice at the sino-tubular junction, ascending and proximal descending aorta both at the level of the pulmonary artery. Rotational flow measurements and derived WSS were averaged over a period at peak systole (one time frame before and three after peak systolic flow) to mitigate measurement noise.⁸

The rotational component of helical flow can be quantified using the ‘circulation’ measure, which is the integral of vorticity with respect to the cross-sectional area of the aorta.^{18, 19} Normal values for rotational flow (‘circulation’) were defined by healthy volunteer controls

(two standard deviations from the mean: -5 to $+11$ mm^2/s). Abnormal (increased) right-handed helical flow (an anti-clockwise rotation viewed from left-anteriorly) was defined as rotational flow values >11 mm^2/s and abnormal left-handed helical flow (clockwise rotation) as <-5 mm^2/s . Complex flow was defined as a lack of an observable coherent helical flow pattern. WSS was calculated using the 3-dimensional flow vector and magnitude data.¹⁶ We measured systolic WSS in eight anatomical positions within the aortic lumen as well as the circumferentially averaged systolic WSS ($\text{WSS}_{\text{circavg}}$) which combined the vector magnitude of both through-plane and in-plane (rotational) WSS.

The systolic flow angle was also calculated – this is the angle between the line perpendicular to the short axis analysis plane and the instantaneous mean flow vector at peak systole (Figure 1B).²⁰

Vascular function measurements

Vascular function measurements were examined to determine any differences in the elastic properties of the aorta consistent with an underlying intrinsic aortopathy. Distensibility (the fractional increase in aortic area as a function of pressure change) was calculated using automated measurements of aortic luminal area.²¹ The maximum rate of systolic distension (MRSD) was calculated as the maximum positive slope (rate of increase) of the normalized lumen area measurements during systole.¹⁰ Pulse wave velocity was computed using in-house software based on widely accepted active contour models²² which automatically segmented 2D phase contrast images, previously validated by Herment et al.²³ The length of the aortic centerline was measured manually on an oblique-sagittal slice through the aorta (half-Fourier single-shot turbo spin-echo [HASTE] scan sequence), while transit time between normalized flow velocity curves was estimated using the half-maximum of the linear fit on the systolic upslope.

Statistical analysis

SPSS Statistics Version 19 (IBM Cooperation, New York, USA) was used for statistical analysis. Data were tested for normal distribution with the Kolmogorov-Smirnov test. Normally distributed data were analyzed using the Students t-test for two group comparison. One-way ANOVA with post-hoc Games-Howell analysis was used for multiple group comparison (e.g. different flow patterns). Correlation was assessed using the Pearson correlation coefficient. Non-normally distributed data were analyzed using non-parametric testing: Mann - Whitney U test for comparison of two groups and Kruskal-Wallis H for multiple group comparison. For categorical data the Chi-square test was performed. A p-value < 0.05 was considered significant.

Results

Patient demographics

One hundred patients with BAV were identified of whom 95 completed the assessment (5 withdrew due to claustrophobia). All 47 healthy volunteers (HV) completed the study protocol successfully. Demographic characteristics and aortic dimensions of the HV and BAV groups are shown in Table 1. The BAV group had larger aortic diameter indexed to BSA at the sinotubular junction and ascending aorta. There was no difference in size at the sinuses of Valsalva, the proximal descending aorta or the distal descending aorta.

Flow patterns in the ascending aorta

Examples of ascending aortic flow patterns in BAV patients are shown in Figure 1, and the distributions among BAV groups in Figure 2. The most common flow pattern was right-handed helical flow, which occurred in 72% of patients ($n=69$). Normal flow patterns were

observed in 11% (n=10), complex flow in 13% (n=12) and left-handed helical flow in 4% (n=4). Aortic dimensions and flow dynamic data are shown in Table 2. BAV patients with right-handed flow patterns had larger ascending aortic diameters, higher systolic flow angles and higher rotational flow values than HV. Those with left-handed flow had even higher values, but the group was too small for meaningful comparison. In contrast, BAV patients with normal flow had similar aortic diameters and systolic flow angles to the HV, but mildly increased rotational flow. The complex flow group had higher ascending aortic diameters and systolic flow angles, but rotational flow values were similar to the HV group, due to the lack of a clearly helical flow pattern. Rotational flow was positively correlated with systolic flow angle ($r=0.240$, $p=0.004$) and strongly correlated with in-plane (rotational) WSS ($r=0.942$, $p<0.001$), as would be expected.

Wall shear stress— WSS_{circavg} was significantly increased in both the right- and left-handed flow groups, predominantly as a result of increased in-plane (rotational) WSS, which contributed over 50% to WSS_{circavg} (<2% in HV). The maximum through-plane WSS was also significantly higher in BAV patients compared to HV, and the right-handed flow group demonstrated marked anterior-posterior eccentricity (difference between outer and inner aortic curvature WSS, Figure 3). The normal flow group had similar in-plane (rotational) WSS values to the HV group, but WSS_{circavg} and maximum through-plane WSS were marginally higher, possibly due to the slightly increased peak velocity from mild aortic valve restriction.

Since WSS is affected by aortic diameter, we attempted to account for this by dividing the group into aortic diameter tertiles: < 15 mm/m², 15 – 22 mm/m² and > 22 mm/m². When comparing these tertiles, the right-handed flow group had significantly higher rotational flow and WSS_{circavg} values throughout compared to the HV group (Figure 4). In the HV, WSS_{circavg} decreased as the aortic diameter enlarged ($p=0.005$) and rotational flow remained at the same low level, whereas WSS_{circavg} remained constant in the right-handed flow group with a slight increase in rotational flow (Figure 4).

Aortic flow patterns in the pediatric population—Comparing the 18 BAV patients aged <18 separately, all forms of flow disturbance were already present and right-handed flow remained the most prevalent pattern (56%), followed by normal flow pattern (28%), left-handed helical flow (11%) and complex flow (5%). One third already had enlarged ascending aortic diameters (z-score >2) and all of these had an abnormal flow pattern despite some having normal aortic valve function. Of the remaining two thirds with normal aortic diameters, 50% already had a right-handed helical flow pattern, even though aortic valve function was normal (n=7) or only mildly stenosed (n=4), suggesting that abnormal flow patterns predate aortic dilation.

Effect of fusion type—The most common fusion type was RL-BAV (58%) followed by RN-BAV (33%). The remaining 9% were left-non coronary fusion (n=3), true anterior-posterior cusp type (n=3) and unicuspid (n=3). The RN-BAV group showed greater flow abnormalities than the RL-BAV group with a normal flow pattern in only 1/31 (3%), left handed helical flow in 10% and complex flow in 23% (Figure 5). We restricted our comparison of hemodynamic flow measures between RL-BAV and RN-BAV to only those with the most common flow abnormality (right-handed flow), in order to minimize the influence of different flow patterns. Both sub-groups were comparable in age, peak velocity, regurgitant fraction and left ventricular function. However the RN-BAV group had larger aortic diameters with more severe hemodynamic flow abnormalities (Table 2). RL-BAV and RN-BAV had a similar systolic WSS profile and eccentricity, but RN-BAV had higher in-plane (rotational) WSS, whereas RL-BAV had a trend towards higher maximum through-

plane WSS and higher anterior-posterior eccentricity (Figure 6). These differences remained significant when patients with aortic stenosis were excluded.

Effect of aortic stenosis on flow abnormalities—Subjects with moderate-severe aortic stenosis had larger ascending aortic diameters, higher positive rotational flow and higher WSS values with more pronounced eccentricity compared to the group with normal valve function or mild aortic stenosis. When comparing stenotic right-handed and left-handed flow patterns, left-handed flow still showed a trend towards higher values (Table 2).

Flow pattern in the descending aorta—The majority of BAV subjects (64%) had a normal flow pattern in the proximal descending aorta (right-handed flow 28%, left-handed flow 8%). There was no difference in diameter of the proximal descending aortic diameter according to flow pattern.

Vascular measures in bicuspid aortic valve disease

There was no substantial difference between the BAV and HV group in all measures of vascular function (Table 3). There were also no significant differences in vascular function measures between any of the BAV sub-groups, and no significant association between vascular function measures and flow patterns when aortic dimensions were taken into account. MRSD was mildly decreased in the BAV group in both the ascending and proximal descending aorta, though with borderline statistical significance for both. Aortic distensibility, arterial strain and MRSD were significantly correlated with age ($r = -0.84, -0.82, -0.79$) and aortic diameter ($r = -0.38, -0.43, -0.58$).

Discussion

Flow abnormalities in bicuspid aortic valve disease

In the largest study to date of 3-dimensional flow patterns in BAV, the most common flow abnormality in the ascending aorta was increased right-handed helical flow, irrespective of the BAV fusion type. Flow abnormalities were most pronounced in the ascending aorta, with a large proportion normalizing in the proximal descending aorta.

The association between flow patterns, wall shear stress and aortic dilation

Even a normally functioning BAV has an asymmetric orifice and increased flow angle compared to HV.²⁴ Our study has shown that this increased flow angle is associated with higher rotational (helical) flow values - the asymmetric jet hits the aortic wall at a more acute angle, resulting in a larger amount of the jet rotating along the aortic wall increasing the in-plane component of the WSS. It also causes asymmetric and locally increased through-plane WSS, which contributes to the increased $WSS_{circavg}$ in BAV. Increased $WSS_{circavg}$ in BAV (particularly with more pronounced helical flow patterns in the ascending aorta) was associated with higher ascending aortic diameters, suggesting that $WSS_{circavg}$ (particularly in-plane [rotational] WSS) may be a causative factor in aortic dilation. While it is not possible to exclude the possibility that the larger ascending aorta leads to increased $WSS_{circavg}$, this would conflict with the findings of previous studies showing reduced WSS in patients with aortic dilation and a tricuspid aortic valve.²⁵ We hypothesise that flow abnormalities initiate the aortopathy as a compensatory response to maintain constant WSS - increased WSS can trigger matrix metalloproteinases and other cellular mechanisms involved in aortic dilation,^{26, 27} and this may be a protective mechanism by which baseline WSS is maintained.²⁶ This is supported by our findings showing lower $WSS_{circavg}$ with increasing aortic diameters in the HV group, but a constant high $WSS_{circavg}$ with increasing aortic diameters in the right-handed flow BAV group.

The concept of abnormal flow patterns and increased WSS occurring prior to aortic dilation (and inferred causal relationship) is also supported by the findings in our pediatric population - several children already showed increased rotational flow values but normal ascending aortic diameters. This is in keeping with a recent study showing increased (visually graded) helical flow in BAV patients without significant valve disease and normal ascending aortic diameters.²⁸ In contrast to BAV patients, patients with Marfan syndrome and known intrinsic aortopathy have essentially normal WSS values in normal sized aortas.²⁹ However, our study and others do not provide conclusive evidence for a causative effect of abnormal flow patterns, but provide supportive data for this hypothesis.

The importance of in-plane (rotational) wall shear stress in aortic dilation and differences between bicuspid aortic valve fusion types

The high proportion of in-plane (rotational) WSS (>50%) in BAV patients seemed to be strongly associated with increased rotational flow and differed between BAV fusion types. The RN-BAV sub-group had increased aortic diameters, systolic flow angles, rotational flow and in-plane WSS, while the RL-BAV group had smaller aortic diameters, and higher maximum through-plane WSS. This might suggest that the higher rotational flow and in-plane WSS contribute to aortic dilation to a greater extent than through-plane WSS and eccentricity. Further studies linking WSS measures and aortic histopathology are needed to further examine this.

The RN-BAV group exhibited more severe flow abnormalities (outlined above, and also including a higher proportion of left-handed flow), and was associated with larger ascending aortic diameters, compared to RL-BAV. While the cause of the dilation in this group is not confirmed (and may reflect either a different intrinsic aortopathy or increased in-plane WSS as discussed above), it suggests that RN-BAV is at higher risk of ascending aortic dilation than the more common RL-BAV, and might be regarded as a marker of poor prognosis. Previous studies examined only small numbers of the RN-BAV sub-group^{8, 17, 28} and the degree of difference in flow patterns between fusion types and association with aortic dimensions had not hitherto been well characterized.

The effect of aortic stenosis

Ascending aortic diameters and degree of stenosis increase with time in subjects with BAV.³⁰ Our study suggests that aortic stenosis further worsens the WSS_{circavg} by: 1) increasing rotational flow and in-plane (rotational) WSS; 2) increasing the maximum through-plane WSS and eccentricity. This is supported by a recent small retrospective study showing higher annual ascending aortic growth rate in BAV subjects with eccentric flow jet compared to those with central flow jets.³¹ However, aortic stenosis does not appear to be the only factor, as high systolic flow angles and rotational flow values were already seen in patients with normally functioning BAV.

Left-handed helical flow

Two previous studies have reported a higher incidence of left-handed flow (10-20%) in young patients with RN-BAV, though numbers were small (n = 5).^{17, 28} We report a similar incidence in the pediatric group, though there was a paucity of left-handed flow patterns in the older BAV population (all our cases were < 26 years old). In all studies, left-handed flow has not been reported in RL-BAV. Our group with left-handed flow was small for meaningful comparison (n=4), but showed a trend towards worse aortopathy, with increased aortic diameters, systolic flow angle, rotational flow and WSS. This may be confounded by coexisting moderate-severe aortic stenosis although flow and WSS values in this group were still increased compared to those with right-handed flow and moderate-severe aortic stenosis. This and the paucity of left-handed flow in the older population might indicate that

a left-handed flow pattern is a more severe abnormality, which may necessitate ascending aortic replacement at a younger age. A larger cohort would be necessary to examine this question in more detail.

Aortic function measures

All measures of aortic function were similar in BAV and HV groups suggesting little evidence of an intrinsic aortopathy, in keeping with one previous echocardiography study.³² This is, however, in contrast to four other echocardiography studies which showed differences in ascending aortic function (e.g. elasticity, distensibility) in mainly younger and smaller BAV cohorts.³³⁻³⁶ These studies also showed larger sinuses of Valsalva, suggesting that these BAV cohorts may have included the aortic root (sinus) dilation phenotype (thought to involve a genetic intrinsic aortopathy⁴ and excluded in our study). This might explain the differences observed. To date, only one study assessed ascending aortic distensibility using CMR in a much younger population (mean age 16 ± 4 years) and showed reduced distensibility and MRS in BAV patients compared to HV.¹⁰

Limitations

This study was cross-sectional in design, and cannot identify causative factors with confidence. A longitudinal study would be more helpful in determining which parameters are predictors for aortic growth and could be used in clinical practice and we plan such a study. The measurement of WSS with 4D flow CMR has relatively low temporal (40ms) and spatial ($\sim 2\text{mm}^3$) resolution¹⁶ and may underestimate the degree of WSS. However, acceptable inter and intra-observer variability were reported in a recent reproducibility study³⁷ and Barker et al. have shown significant results even after adjusting for a maximum error of 10%.⁸ We specifically targeted the RN-BAV sub-type for recruitment, as previous studies had difficulty in finding significant numbers. The proportion of the different fusion types in our cohort does not therefore reflect the distribution in the general BAV population.

Conclusion

Our study suggests that hemodynamic flow abnormalities caused by BAV are associated with ascending aortic dilation and may be an important etiological factor in the pathogenesis of this condition. We cannot provide conclusive evidence for a causative effect of flow abnormalities on aortic dilation however, and longitudinal follow up studies would provide further insight. We also demonstrated variation in the severity of flow abnormalities and aortic dilation among different BAV fusion types, and this may facilitate risk stratification in BAV aortopathy. These findings further our understanding of the aortopathy associated with BAV, and may allow future selection of patients who benefit from intensified follow up and earlier surgical intervention.

Acknowledgments

We would like to thank Karen Whatley and Christine Saward for their work with the OXBAV database.

Sources of Funding

This study was funded by a British Heart Foundation Clinical Research Training Fellowship (Dr. Bissell). Dr Hess is supported by the Medical Research Council. Dr Biasioli is supported by the Engineering and Physical Sciences Research Council. Dr. Pitcher has received funding support from the British Heart Foundation. Prof Markl is supported by NIH National Heart, Lung, and Blood Institute grant R01HL115828, Northwestern University Clinical and Transitional Sciences Institute NIH grant UL1RR025741, and the Northwestern Memorial Foundation Dixon Translational Research Grants Initiative. Dr Barker is supported by the American Heart Association Scientist Development Grant 13SDG14360004. Prof Neubauer is supported by the Oxford Biomedical Research Centre and National Institute for Health Research and acknowledges support from the British Heart

Foundation Centre of Research Excellence. Dr. Myerson and Dr Prendergast are supported by the Oxford Biomedical Research Centre, with UK National Institute for Health Research funding.

References

1. Ward C. Clinical significance of the bicuspid aortic valve. *Heart*. 2000; 83:81–85. [PubMed: 10618341]
2. Sievers HH, Sievers HL. Aortopathy in bicuspid aortic valve disease - genes or hemodynamics? or Scylla and Charybdis? *Eur J Cardiothorac Surg*. 2011; 39:803–804. [PubMed: 21459598]
3. Loscalzo ML, Goh DL, Loeys B, Kent KC, Spevak PJ, Dietz HC. Familial thoracic aortic dilation and bicommissural aortic valve: a prospective analysis of natural history and inheritance. *Am J Med Genet A*. 2007; 143A:1960–1967. [PubMed: 17676603]
4. Girdauskas E, Borger MA, Secknus MA, Girdauskas G, Kuntze T. Is aortopathy in bicuspid aortic valve disease a congenital defect or a result of abnormal hemodynamics? A critical reappraisal of a one-sided argument. *Eur J Cardiothorac Surg*. 2011; 39:809–814. [PubMed: 21342769]
5. Fernandez B, Duran AC, Fernandez-Gallego T, Fernandez MC, Such M, Arque JM, Sans-Coma V. Bicuspid aortic valves with different spatial orientations of the leaflets are distinct etiological entities. *J Am Coll Cardiol*. 2009; 54:2312–2318. [PubMed: 19958967]
6. Schaefer BM, Lewin MB, Stout KK, Byers PH, Otto CM. Usefulness of bicuspid aortic valve phenotype to predict elastic properties of the ascending aorta. *Am J Cardiol*. 2007; 99:686–690. [PubMed: 17317372]
7. Hope MD, Hope TA, Crook SE, Ordovas KG, Urbania TH, Alley MT, Higgins CB. 4D flow CMR in assessment of valve-related ascending aortic disease. *JACC Cardiovasc Imaging*. 2011; 4:781–787. [PubMed: 21757170]
8. Barker AJ, Markl M, Burk J, Lorenz R, Bock J, Bauer S, Schulz-Menger J, von Knobelsdorff-Brenkenhoff F. Bicuspid aortic valve is associated with altered wall shear stress in the ascending aorta. *Circ Cardiovasc Imaging*. 2012; 5:457–466. [PubMed: 22730420]
9. Sievers HH, Schmidtke C. A classification system for the bicuspid aortic valve from 304 surgical specimens. *J Thorac Cardiovasc Surg*. 2007; 133:1226–1233. [PubMed: 17467434]
10. Donato Aquaro G, Ait-Ali L, Basso ML, Lombardi M, Pingitore A, Festa P. Elastic properties of aortic wall in patients with bicuspid aortic valve by magnetic resonance imaging. *Am J Cardiol*. 2011; 108:81–87. [PubMed: 21529726]
11. Burman ED, Keegan J, Kilner PJ. Aortic root measurement by cardiovascular magnetic resonance: specification of planes and lines of measurement and corresponding normal values. *Circ Cardiovasc Imaging*. 2008; 1:104–113. [PubMed: 19808527]
12. Haycock GB, Schwartz GJ, Wisotsky DH. Geometric method for measuring body surface area: a height-weight formula validated in infants, children, and adults. *J Pediatr*. 1978; 93:62–66. [PubMed: 650346]
13. Pucci G, Cherian J, Hubsch A, Hickson SS, Gajendragadkar PR, Watson T, O'sullivan M, Woodcock-Smith J, Schillaci G, Wilkinson IB, McEniery CM. Evaluation of the Vicorder, a novel cuff-based device for the noninvasive estimation of central blood pressure. *J Hypertens*. 2013; 31:77–85. [PubMed: 23079681]
14. Markl M, Harloff A, Bley TA, Zaitsev M, Jung B, Weigang E, Langer M, Hennig J, Frydrychowicz A. Time-resolved 3D MR velocity mapping at 3T: improved navigator-gated assessment of vascular anatomy and blood flow. *J Magn Reson Imaging*. 2007; 25:824–831. [PubMed: 17345635]
15. Frydrychowicz A, Harloff A, Jung B, Zaitsev M, Weigang E, Bley TA, Langer M, Hennig J, Markl M. Time-resolved, 3-dimensional magnetic resonance flow analysis at 3 T: visualization of normal and pathological aortic vascular hemodynamics. *J Comput Assist Tomogr*. 2007; 31:9–15. [PubMed: 17259827]
16. Stalder AF, Russe MF, Frydrychowicz A, Bock J, Hennig J, Markl M. Quantitative 2D and 3D phase contrast MRI: optimized analysis of blood flow and vessel wall parameters. *Magn Reson Med*. 2008; 60:1218–1231. [PubMed: 18956416]

17. Hope MD, Hope TA, Meadows AK, Ordovas KG, Urbania TH, Alley MT, Higgins CB. Bicuspid aortic valve: four-dimensional MR evaluation of ascending aortic systolic flow patterns. *Radiology*. 2010; 255:53–61. [PubMed: 20308444]
18. Farthing S, Peronneau P. Flow in the thoracic aorta. *Cardiovasc Res*. 1979; 13:607–620. [PubMed: 519664]
19. Hess AT, Bissell MM, Glaze SJ, Pitcher A, Myerson SG, Neubauer S, Robson MD. Evaluation of Circulation as a quantifying metric in 4D flow MRI. *J Cardiovasc Magn Reson*. 2013; 15(Suppl1):E36.
20. Entezari P, Schnell S, Mahadevia R, Rinewalt D, Malaisrie C, McCarthy P, Collins J, Carr JC, Markl M, Barker AJ. From unicuspid to quadricuspid: The impact of aortic valve morphology on 3D hemodynamics. *J Cardiovasc Magn Reson*. 2013; 15(Suppl1):O79.
21. Jackson CE, Shirodaria CC, Lee JM, Francis JM, Choudhury RP, Channon KM, Noble JA, Neubauer S, Robson MD. Reproducibility and accuracy of automated measurement for dynamic arterial lumen area by cardiovascular magnetic resonance. *Int J Cardiovasc Imaging*. 2009; 25:797–808. [PubMed: 19779977]
22. Kass M, Witkin A, Terzopoulos D. Snakes: Active contour models. *Int J Comput Vision*. 1988; 1:321–331.
23. Herment A, Kachenoura N, Lefort M, Bensalah M, Dogui A, Frouin F, Mousseaux E, De Cesare A. Automated segmentation of the aorta from phase contrast MR images: validation against expert tracing in healthy volunteers and in patients with a dilated aorta. *J Magn Reson Imaging*. 2010; 31:881–888. [PubMed: 20373432]
24. Della Corte A, Bancone C, Conti CA, Votta E, Redaelli A, Del Viscovo L, Cotrufo M. Restricted cusp motion in right-left type of bicuspid aortic valves: a new risk marker for aortopathy. *J Thorac Cardiovasc Surg*. 2012; 144:360–9. 369.e1. [PubMed: 22050982]
25. Burk J, Blanke P, Stankovic Z, Barker A, Russe M, Geiger J, Frydrychowicz A, Langer M, Markl M. Evaluation of 3D blood flow patterns and wall shear stress in the normal and dilated thoracic aorta using flow-sensitive 4D CMR. *J Cardiovasc Magn Reson*. 2012; 14:84. 429X-14-84. [PubMed: 23237187]
26. Lehoux S, Tedgui A. Cellular mechanics and gene expression in blood vessels. *J Biomech*. 2003; 36:631–643. [PubMed: 12694993]
27. Ruddy JM, Jones JA, Stroud RE, Mukherjee R, Spinale FG, Ikonomidis JS. Differential effect of wall tension on matrix metalloproteinase promoter activation in the thoracic aorta. *J Surg Res*. 2010; 160:333–339. [PubMed: 19375723]
28. Meierhofer C, Schneider EP, Lyko C, Hutter A, Martinoff S, Markl M, Hager A, Hess J, Stern H, Fratz S. Wall shear stress and flow patterns in the ascending aorta in patients with bicuspid aortic valves differ significantly from tricuspid aortic valves: a prospective study. *Eur Heart J Cardiovasc Imaging*. 2012 Dec 9. Epub ahead of print.
29. Geiger J, Arnold R, Herzer L, Hirtler D, Stankovic Z, Russe M, Langer M, Markl M. Aortic wall shear stress in Marfan syndrome. *Magn Reson Med*. 2012 Nov 20. Epub ahead of print. 10.1002/mrm.24562
30. Michelena HI, Desjardins VA, Avierinos JF, Russo A, Nkomo VT, Sundt TM, Pellicka PA, Tajik AJ, Enriquez-Sarano M. Natural history of asymptomatic patients with normally functioning or minimally dysfunctional bicuspid aortic valve in the community. *Circulation*. 2008; 117:2776–2784. [PubMed: 18506017]
31. Hope MD, Wrenn J, Sigovan M, Foster E, Tseng EE, Saloner D. Imaging biomarkers of aortic disease: increased growth rates with eccentric systolic flow. *J Am Coll Cardiol*. 2012; 60:356–357. [PubMed: 22813616]
32. Yap SC, Nemes A, Meijboom FJ, Galema TW, Geleijnse ML, ten Cate FJ, Simoons ML, Roos-Hesselink JW. Abnormal aortic elastic properties in adults with congenital valvular aortic stenosis. *Int J Cardiol*. 2008; 128:336–341. [PubMed: 17689754]
33. Bilen E, Akcay M, Bayram NA, Kocak U, Kurt M, Tanboga IH, Bozkurt E. Aortic elastic properties and left ventricular diastolic function in patients with isolated bicuspid aortic valve. *J Heart Valve Dis*. 2012; 21:189–194. [PubMed: 22645854]

34. Nistri S, Grande-Allen J, Noale M, Basso C, Siviero P, Maggi S, Crepaldi G, Thiene G. Aortic elasticity and size in bicuspid aortic valve syndrome. *Eur Heart J*. 2008; 29:472–479. [PubMed: 18096569]
35. Oulego-Erroz I, Alonso-Quintela P, Mora-Matilla M, Gautreaux Minaya S, Lapena-Lopez de Armentia S. Ascending aorta elasticity in children with isolated bicuspid aortic valve. *Int J Cardiol*. 2012 Dec 8. Epub ahead of print. 10.1016/j.ijcard.2012.11.080
36. Santaripa G, Scognamiglio G, Di Salvo G, D'Alto M, Sarubbi B, Romeo E, Indolfi C, Cotrufo M, Calabro R. Aortic and left ventricular remodeling in patients with bicuspid aortic valve without significant valvular dysfunction: a prospective study. *Int J Cardiol*. 2012; 158:347–352. [PubMed: 21315467]
37. Markl M, Wallis W, Harloff A. Reproducibility of flow and wall shear stress analysis using flow-sensitive four-dimensional MRI. *J Magn Reson Imaging*. 2011; 33:988–994. [PubMed: 21448968]

Clinical perspective summary

Bicuspid aortic valve disease (BAV) is the most common congenital heart condition, and the associated aortic dilation in particular can require lifelong follow-up. Understanding more about the aortic pathophysiology is important for identifying future risk, which could potentially facilitate efficient use of healthcare resources and patient time. The need for frequent follow-up may be reduced in patients with a low risk of aortic dilation, while concentrating the focus on those at high risk. We have shown that the most common cusp fusion sub-type (right-left coronary cusp fusion) has lesser degrees of flow disturbance, with some patients even having normal flow profiles. In contrast the rarer right-non coronary cusp fusion group not only has a more pronounced flow disturbance and larger aortic diameters, but also has a higher incidence of left-handed flow disturbances and may benefit from more frequent follow-up. The distinction of these two groups can be made on echocardiography or a standard clinical CMR scan.

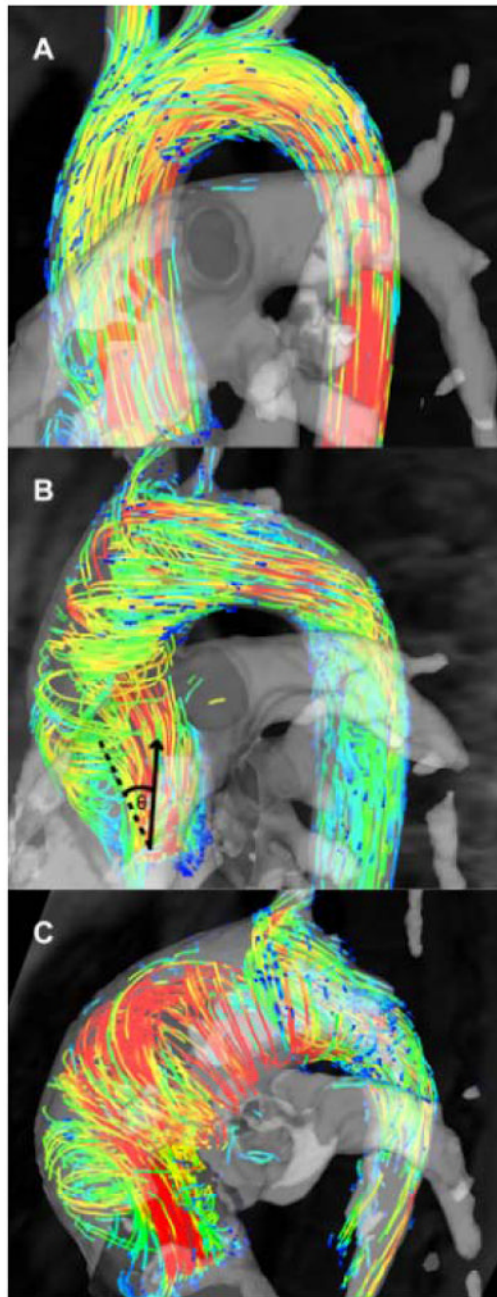


Figure 1. Flow patterns in bicuspid aortic valve disease; (A) Normal flow pattern; (B) Right-handed helical flow; (C) Left-handed helical flow. The systolic flow angle (θ) is demonstrated on Figure B - the angle between the aortic mid-line (dashed) and the instantaneous mean flow vector at peak systole (arrow).

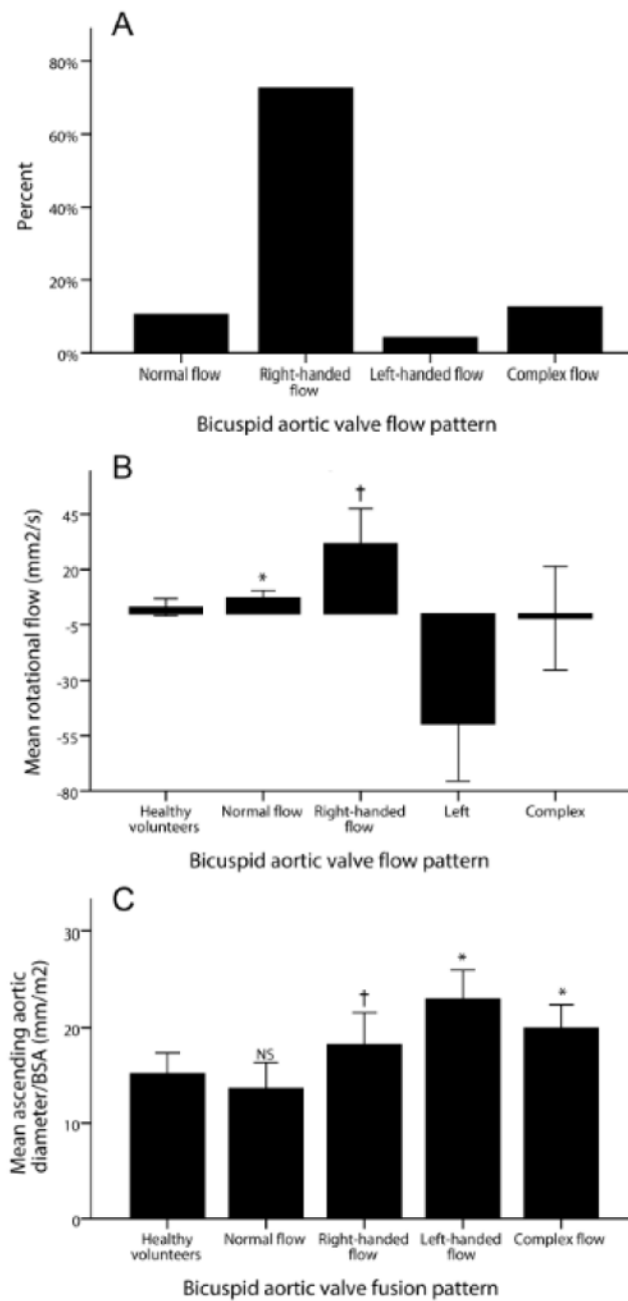


Figure 2.

(A) Incidence of flow patterns in bicuspid aortic valve disease (BAV); (B) Mean rotational flow values in the different BAV flow patterns; (C) Mean ascending aortic diameter in the different flow patterns; Error bars indicate standard deviation; * $p < 0.05$ compared to healthy volunteers (HV); † $p < 0.001$ compared to HV

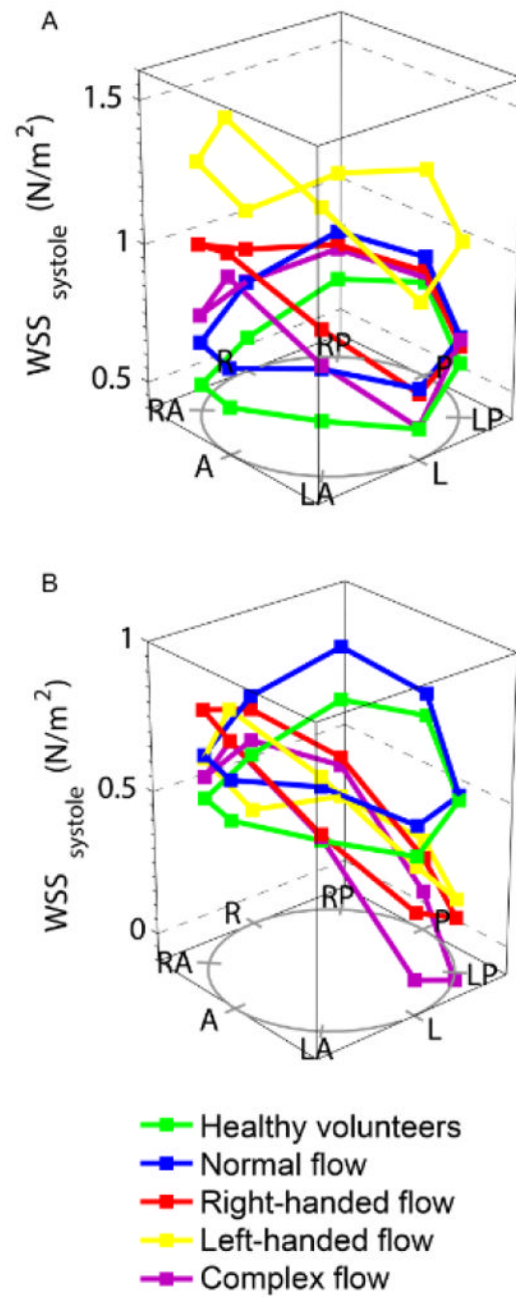


Figure 3. Wall shear stress (WSS) at all locations in the ascending aorta, in different bicuspid aortic valve flow patterns; (A) systolic WSS; (B) through-plane systolic WSS. A= anterior, LA= left anterior, L= left, LP= left posterior, P= posterior, RP= right posterior, R= right, RA= right anterior

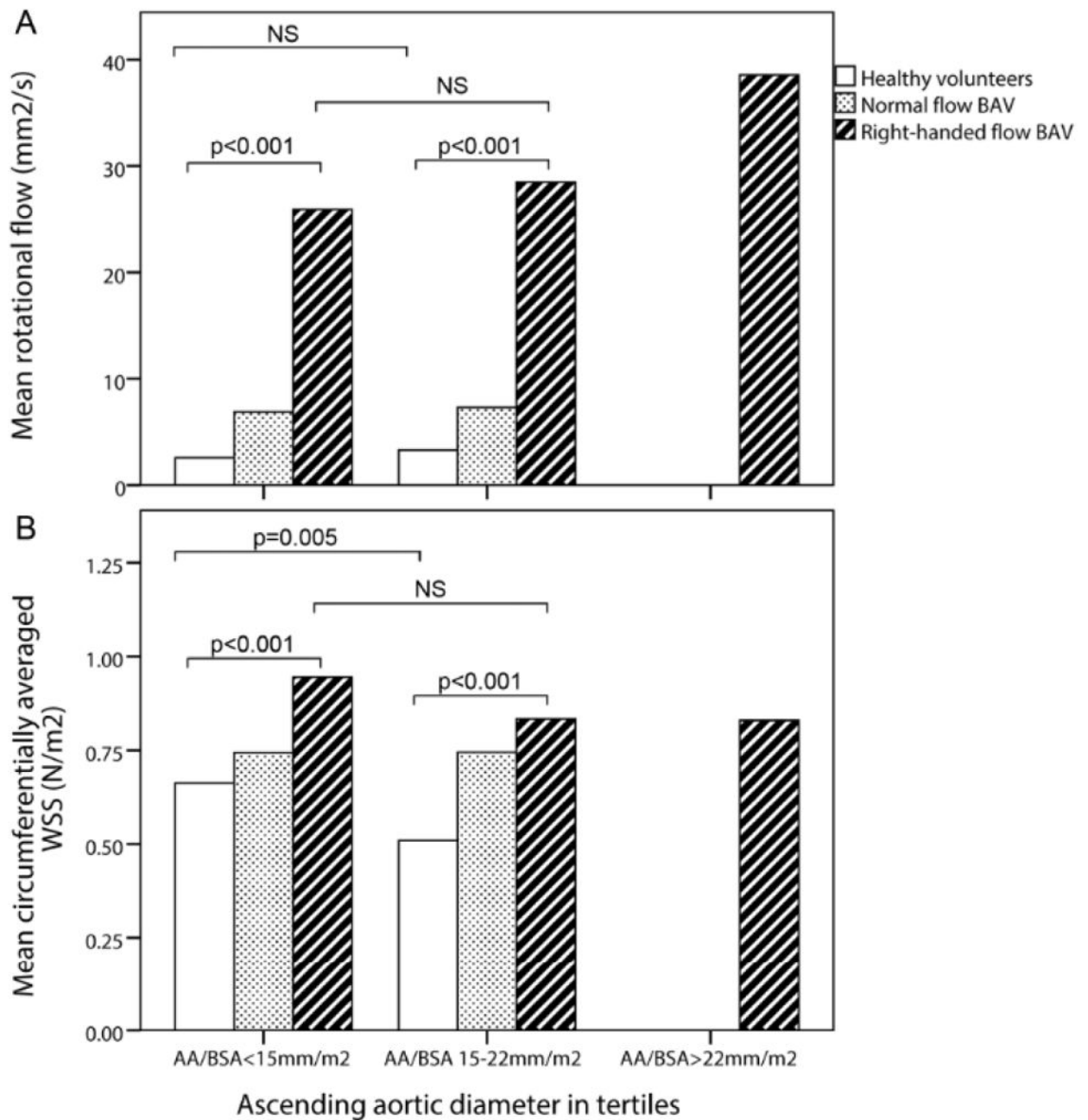


Figure 4. Mean rotational flow (a) and peak systolic circumferentially-averaged wall shear stress (WSS) (b) in ascending aortic diameter tertiles; NS = not significant; AA/BSA = ascending aortic diameter/Body surface area

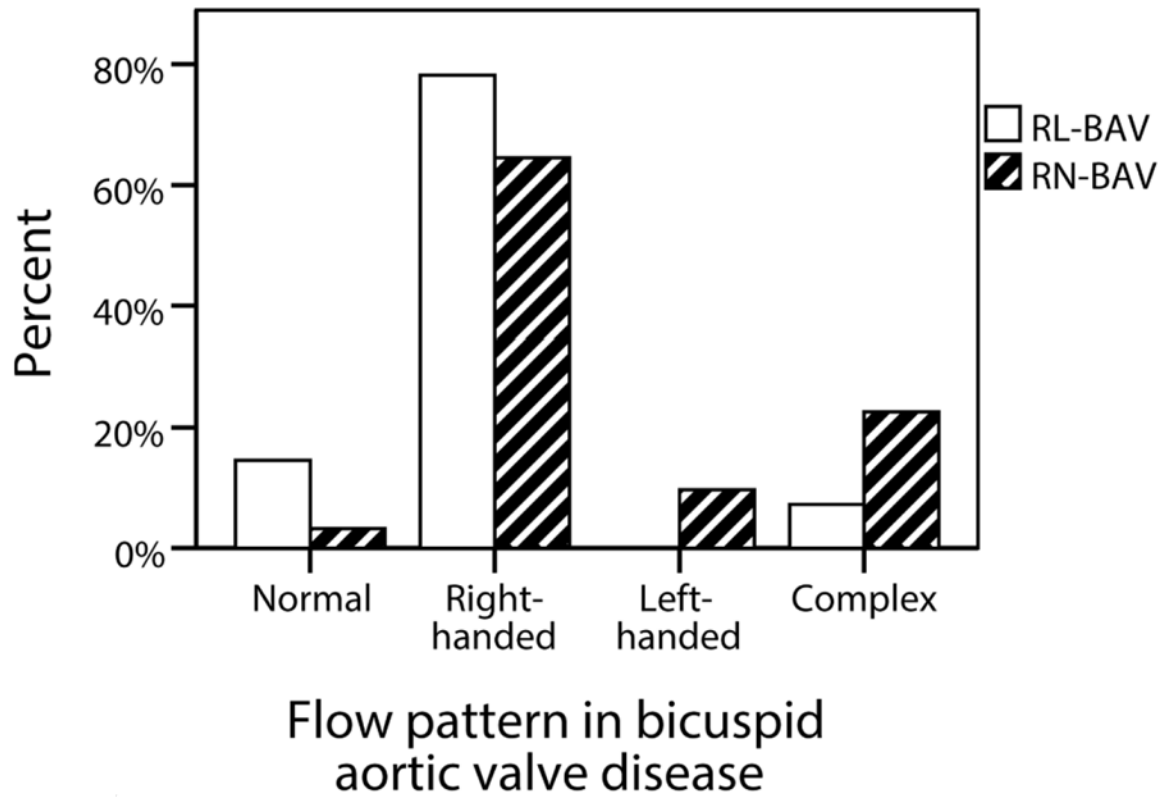


Figure 5. Proportion of patients with each ascending aortic flow pattern in the two main bicuspid aortic valve fusion sub-groups (RL-BAV and RN-BAV)

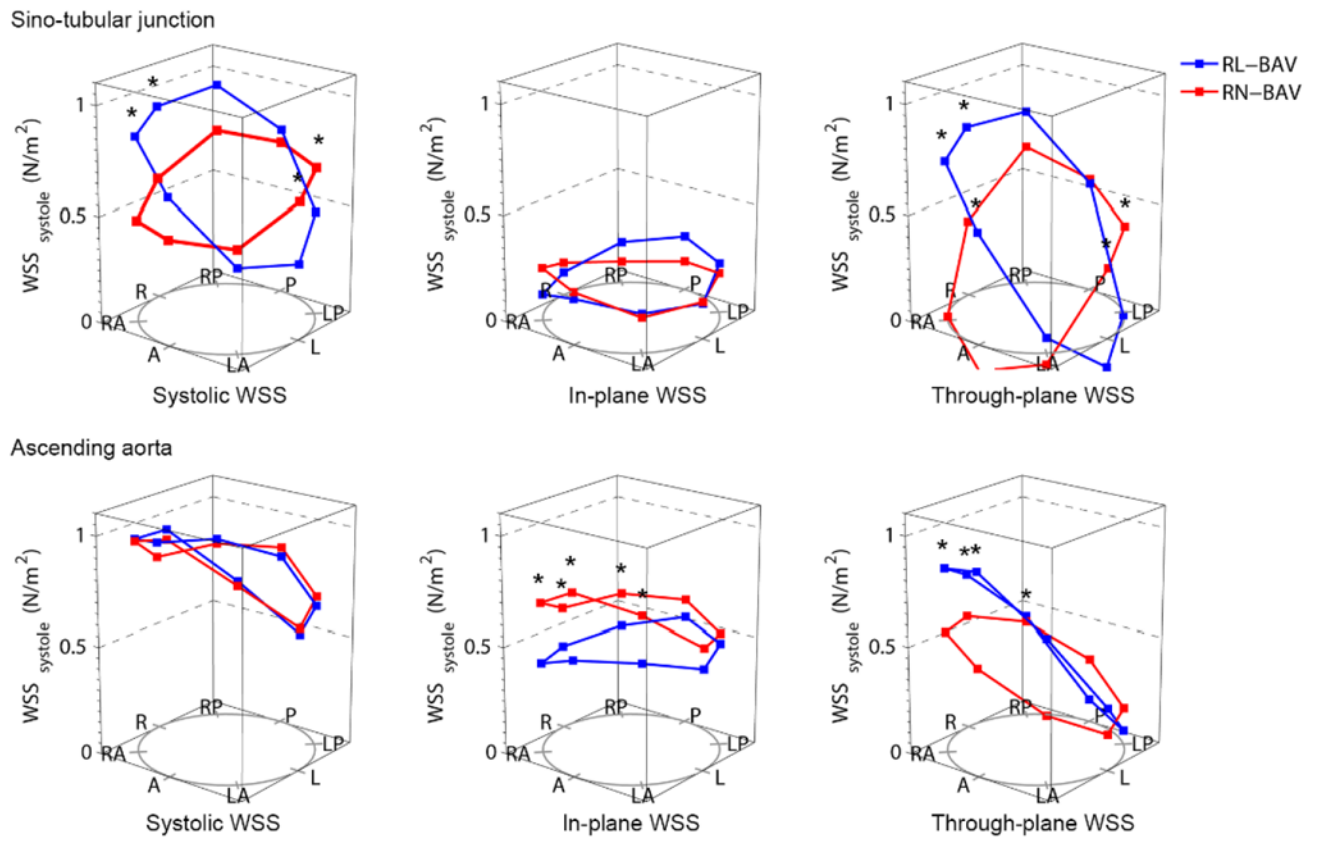


Figure 6. Wall shear stress (WSS) profiles in the leaflet fusion groups (RL-BAV and RN-BAV) with right-handed helical flow; Abbreviations as for Figure 3; *= p<0.05

Table 1

Demographics and aortic dimensions of healthy volunteers and patients with bicuspid aortic valve disease

	Healthy volunteers	Bicuspid aortic valve patients
Male (%)	68%	76%
Age (years)	40.2±17.7	39.5±16.9
Mean arterial pressure (mmHg)	87.9±11.1	89.2±12.0
Aortic diameters/BSA (mm/m ²):		
<i>Aortic sinuses</i>	16.7±2.2	17.2±2.7
<i>Sinotubular junction</i>	15.1±2.1	16.6±3.1*
<i>Mid ascending aorta</i>	15.2±2.2	18.2±3.7*
<i>Proximal descending aorta</i>	11.0±1.6	11.2±1.8
<i>Distal descending aorta</i>	9.8±1.5	9.8±1.6

Values are mean ±standard deviation;

*
p<0.001;

BSA = body surface area

Table 2
Aortic dimensions and flow hemodynamics in bicuspid aortic valve disease and healthy volunteers

	Healthy volunteers (n=47)			Bicuspid aortic valve patients (all fusion types)			BAV fusion sub-types (right-handed flow only)			Aortic stenosis types	
	Normal flow (n=10)	Right-handed flow (n=69)	Left-handed flow (n=4)	Complex flow (n=12)	RL-BAV (n=43)	RN-BAV (n=20)	Aortic stenosis (n=24)	No aortic stenosis (n=71)			
Aortic diameter/BSA (mm/m ²)	15.1±2.1	16.5±3.1*	19.1±1.6	18.2±2.9*	16.2±3.4	17.4±2.4	17.3±2.4	16.3±3.3			
<i>Sinotubular junction</i>	15.2±2.2	18.3±3.3**	23.0±3.1*	20.0±2.5***	17.5±3.1	19.5±3.4†	19.9±2.1	17.6±3.9††			
<i>Mid ascending aorta</i>	7.0±4.6	23.1±12.5***	30.0±16.1	30.0±11.6**	19.4±11.4	29.4±10.9††	27.1±11.3	21.7±13.5			
Systolic flow angle (°)	2.9±3.9	31.7±15.8**	-49.7±25.8	-2.0±23.4	27.8±12.4	38.5±16.5†††	41.1±23.5	23.4±13.5†††			
Rotational flow (mm ² /m)	0.59±0.17	0.85±0.28**	1.18±0.29	0.76±0.25	0.85±0.25	0.84±0.31	1.09±0.28	0.76±0.21†††			
Systolic WSS _{circavg} (N/m ²)	0.01±0.12	0.53±0.24**	-0.84±0.35	-0.01±0.40	0.47±0.22	0.64±0.23†††	0.65±0.35	0.41±0.23†††			
Systolic in-plane WSS (N/m ²)	0.75±0.20	1.02±0.45**	1.31±0.53	1.05±0.49	1.05±0.38	0.88±0.49	1.47±0.48	0.89±0.31†††			
max systolic through-plane WSS (N/m ²)	-0.18±0.17	0.32±0.44**	0.40±0.48	0.26±0.51	0.30±0.57	-0.07±0.56†	0.70±0.48	0.12±0.36†††			
Anterior - posterior eccentricity (N/m ²)	n/a	2.5±0.8	3.7±0.5	3.2±1.0	2.4±0.7	2.5±0.8	3.9±0.5	2.1±0.4†††			
Peak velocity (m/sec)	40.2±17.7	24.1±11.5*	42.2±17.1	42.7±17.5	42.0±15.5	43.9±17.2	39.5±18.9	39.4±16.3			
Age (years)											

Values are mean ±standard deviation;

* p<0.05,

** p<0.001 vs. healthy volunteers;

† p<0.05,

†† p<0.001 comparing BAV fusion sub-types,

‡ p<0.05,

‡‡ p<0.001 comparing aortic stenosis sub-types;

BSA =body surface area; max= maximum

Table 3
Aortic vascular function measures in healthy volunteers and patients with bicuspid aortic valve disease

	Healthy volunteers	Bicuspid aortic valve patients
Distensibility (1 / mmHg):		
Ascending aorta	4.65±3.21	4.06±3.07
Proximal descending aorta	4.86±2.05	4.98±2.28
Distal descending aorta	7.31±3.49	7.65±4.12
Arterial strain:		
Ascending aorta	0.21±0.13	0.19±0.13
Proximal descending aorta	0.23±0.09	0.24±0.10
Distal descending aorta	0.33±0.13	0.37±0.18
Maximum rate of systolic distension (%/ms):		
Ascending aorta	0.20±0.11	0.16±0.10*
Proximal descending aorta	0.21±0.09	0.18±0.08*
Distal descending aorta	0.27±0.07	0.24±0.08
Median pulse wave velocity arch (range) (m/s)	4.74 (13.05)	4.54 (29.67)
Median central pulse pressure (range) mmHg	47 (37)	51 (43)*

Values are mean ±standard deviation or median (range);

SE = standard error;

* p=0.04